# COMPENSATION EFFECT IN CATALYTIC HYDROLYSIS OF CARBONYL SULFIDE AT LOWER TEMPERATURE
# COMPENSATION EFFECT IN COS HYDROLYSIS

TAN Shishao, LI Chunhu, LIANG Shengzhao and GUO Hanxian

*Department of Chemical Engineering, Taiyuan University of Technology, Taiyuan, Shanxi, 030024, China*

Received 24 January 1990; accepted 10 December 1990

A series of catalysts impregnated with alkali metal oxides and alkali earth metal oxides for COS hydrolysis reaction was prepared. The activities of catalysts in lower temperature range (45–100 °C) were investigated by means of microreactor-chromatograph. It was shown that the catalytic activity is closely related to the oxide and its content. Further, it was also observed that a compensation effect exists by studying the reaction rate constant ($k$) at various temperatures. That is, the activation energy ($E$) increases along with the increase of the pre-exponential factor ($A$).

Both compensation effect parameter ($K_0$) and energy distribution exponential factor ($1/b$) are closely related to the metal ionic radius ($d_m$).

$K_0 = 11.437 - 6.5189\, d_m$, $\ln(1/b) = \ln 2.6382 + 0.039577 \ln K_0$.

The isokinetic temperatures ($T_s$) of all prepared catalysts were obtained. A possible explanation for the compensation effect in COS hydrolysis was given.

**Keywords:** Carbon oxide sulfide, compensation effect, catalysis, alumina, hydrolysis

## 1. Introduction

Carbonyl sulfide (COS) widely exists in chemical processing gases from coal, Claus tail gas, petroleum and natural gas. Since it is difficult to remove COS completely by the conventional desulfurization process, a hydrolysis process has been developed in recent years.

$$COS + H_2O = CO_2 + H_2S.$$

The early studies mainly concentrated on the treatment of Claus tail gas to meet the requirements of environmental protection. Almost all the studies were carried out in higher temperature range (above 200 °C) [1–4].

In previous publications from this laboratory [5,6], the kinetics of carbonyl sulfide hydrolysis, the characteristic and mechanism of deactivation were investigated over a commercial $\gamma$-$Al_2O_3$ catalyst in lower temperature range. It was

shown that the time of deactivation of $Al_2O_3$ is only 2 hours, and catalyst activity decreases dramatically with the increase of the reaction temperature and oxygen content in feed stream. Furthermore, the catalyst basicity increases the rate for COS hydrolysis.

An attempt was made to study the behavior of $\gamma$-$Al_2O_3$ doped with alkali metal oxides and alkali earth metal oxides at lower temperature. The results are summarized in this report.

## 2. Experimental methods

### CATALYST PREPARATION

The $\gamma$-$Al_2O_3$ was manufactured by the Shenyang Catalyst Plant, its surface area is 203 $m^2/g$. The chemicals used are all A.R. grade.

The $\gamma$-$Al_2O_3$ extrudates approximately 3 * 5 mm in size were impregnated to incipient wetness with an aqueous solution. The volume of the solution used was equal to the product of water absorption and weight of the $\gamma$-$Al_2O_3$. The saturated extrudates were kept humid over night at room temperature, dried at 120 ° C for 2 hours and calcined at 550 ° C for 2 hours. By varying the component and concentration of the solution respectively, a series of catalysts was prepared.

The catalysts were crashed and sieved to 40–60 mesh granules for kinetics studies.

### REACTANTS

COS was prepared by the reaction of saturated solution of potassium thiocyanate with 50% (wt./wt.) sulfuric acid at 30 ° C [7]. As KCNS was added dropwise to $H_2SO_4$, the following reaction occurs:

$$KCNS + 2H_2SO_4 + H_2O = KHSO_4 + NH_4HSO_4 + COS.$$

There are some side products such as $CO_2$, $SO_2$, HCOOH, $H_2S$ and HCN. Therefore, the outflow gas was purified by treatments first with a mixture of saturated aqueous $CuSO_4$ solution and concentrated $H_2SO_4$ (50%, volume ratio) to remove $H_2S$, and a 30% aqueous KOH solution to remove acid gases. This then was followed by a 25% solution of aniling in alcohol to remove the $CS_2$, and by concentrated $H_2SO_4$ to remove $H_2O$ [7].

The COS was sampled and analysed several times using GC (SP2305E chromatograph equipped with TCD). A 4 m * 4 mm (o.d.) stainless steel column packed with GD-303 was used for detecting the impurities. No other peak was found. Then the COS was filled in compressed gas cylinders made of glass fibre reinforced plastics with nitrogen as balance gas. Thus the concentration of COS was about 100–200 ppm.

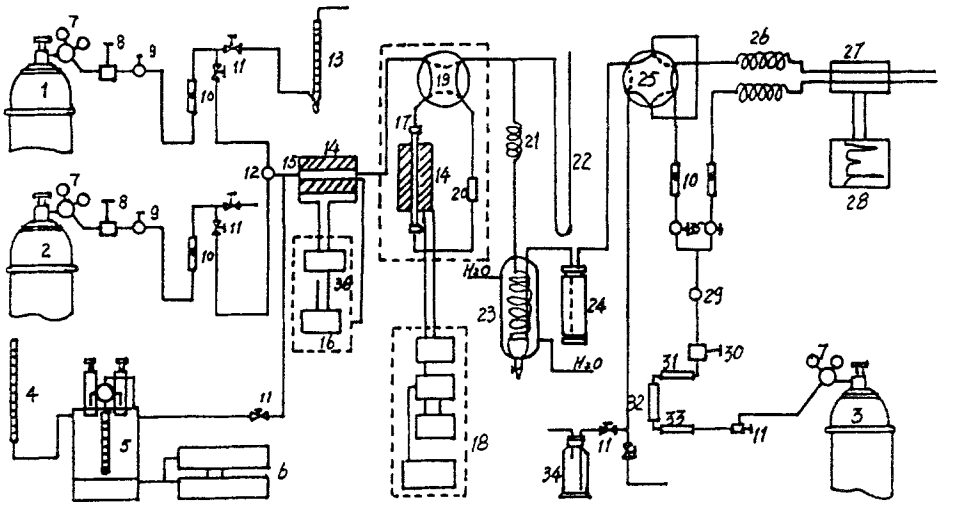

Fig. 1. Schematic diagram of apparatus. 1, $N_2$; 2, COS; 3, $H_2$; 4, water; 5, syringe pump; 6, pump controller; 7, pressure gauge; 8, steady flow valve; 9, micro adjuster; 10, flow meter; 11, switch valve; 12, three way; 13, soap flow meter; 14, furnace; 15, mixer; 16, temperature controller; 17, reactor; 18, temperature programmer; 19, four way; 20, filter; 21, cooling tuber; 22, pressure meter; 23, water cooler; 24, $H_2S$ absorber; 25, six way; 26, GC column; 27, FPD; 28, recorder; 29, pressure meter; 30, steady flow valve; 31, purifier; 32, silica gel drier; 33, $O_2$-removing tube; 34, COS absorber; 35, needle valve; 36, pressure regulator

The necessary precautions were taken during the preparation and handling of COS.

The distilled water was fed via a syringe pump.

## APPARATUS

A microreactor-chromatograph was used in this study, see fig. 1.

The reactor was made of stainless steel. The diameter of the catalyst bed was 6 mm and the diameter of the surrounding thermal constant block was 40 mm. A thermocouple was located approximately in the centre of the catalyst bed. The furnace was controlled by a PID and CGQ-01 temperature programmer. The thermocouple output could be read to $\pm 0.5\,^{\circ}C$.

The Shimadzu GC-9A gas chromatograph equipped with a duel flame FPD was used in this study. A 4 m * 4 mm (o.d.) stainless steel column packed with GDX-300 was used for all measurements. Conversion and yield were calculated on the basis of the material balance of COS, such as:

$$X = (C_0 - C)/C_0\% \tag{1}$$

where

$X$ : Conversion of COS

$C_0$ : Inlet concentration of COS

$C$ : Outlet concentration of COS.

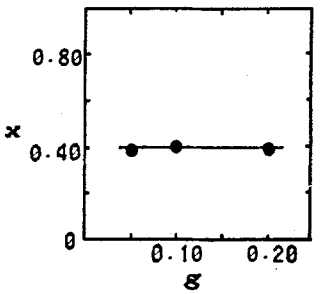


Fig. 2. Test of film diffusion. Catalyst weight (g) vs. COS conversion ($X$); catalyst: 4% (wt.%) $K_2O/\gamma$-$Al_2O_3$, 40–60 mesh; reaction temp.: 80 °C; space velocity: 20000 $h^{-1}$; $H_2O/COS > 100$.

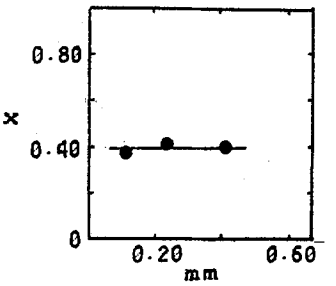


Fig. 3. Test of pore diffusion. Catalyst size (mm) vs. COS conversion ($X$); catalyst: 4% (wt.) $K_2O/\gamma - Al_2O_3$, 0.1 g; reaction temp.: 80 °C; space velocity: 20000 $h^{-1}$; $H_2O/COS$: > 100.

## OPERATION OF EQUIPMENT

The temperature profile of the reactor shows that there is a 30 mm isothermal region. The preliminary experiments with the reactor filled with $SiO_2$ at several temperatures show that the reactor itself could not promote COS hydrolysis. Also, film and pore diffusion tests were carried out using 4% (wt.%) $K_2O/\gamma$-$Al_2O_3$ as catalyst at constant space velocity, see figs. 2, 3. As the conversion does not change with the catalyst weight or with changes in the particle dimensions, possible film or pore diffusion were not considered to be rate determining steps under the operation condition. This was assumed to hold true for the other catalysts as well. In this study, the size of the catalyst was 0.24 mm (40–60 mesh) and the catalyst weight was 0.1 g. When $H_2O/COS$ was less then 5, the conversion of COS increased as $H_2O/COS$ raised. $H_2O$ was first order. When $H_2O/COS$ was larger than 5, increasing the $H_2O/COS$ could not change the conversion of COS, the reaction order of $H_2O$ became zero, see fig. 4. Similar results had been reported by others at higher temperature [4]. In this study the $H_2O/COS$ was larger than 100.

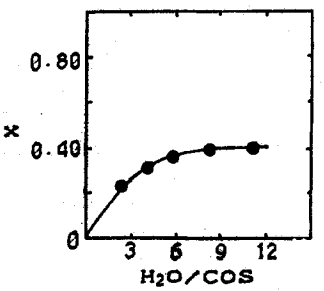


Fig. 4. Influence of $H_2O/COS$ on COS conversion. Catalyst: $\gamma$-$Al_2O_3$, 40–60 mesh, 0.1 g; reaction temp.: 55 °C; space velocity: 20000 $h^{-1}$.

Thus, the experimental conditions were selected. As the COS concentration is only about 100–200 ppm, the temperature-difference effects caused by the heat of reaction both within the particle, and outside it, will probably be small. Considering the relatively long isothermal region (30 mm) within the reactor and the large space velocity (20000 $h^{-1}$) employed, we may assume that it is an ideal isothermal plug-flow reactor without considerable deviation.

After complete purging of air from the reactor with nitrogen at room temperature, the reactor was heated to the reaction temperature (45–80 °C). Steady state condition was usually established after a preliminary period of about 1 hour, as indicated by constant COS conversions.

## 3. Results and discussion

### KINETIC STUDIES

The hydrolysis of carbonyl sulfide shows first-order behavior for COS, as it was reported by several researchers over different reaction systems [1–5]. Thus we have

$$-dC/dt = KC \tag{2}$$

where

$K$ : Reaction rate constant ($sec^{-1}$)

$C$ : Concentration of COS

$t$ : Contact time (sec)

when $t = 0$, $C = C_0$; $t = t$, $C = C$. For an ideal isothermal plug-flow reactor, we have the integral form of [2].

$$\ln(C_0/C) = Kt \tag{3}$$

from (1) and (3) we have

$$K = -[\ln(1 - X)]/t \tag{4}$$

$V_{sp}$ is the space velocity of COS gas stream. In this study $V_{sp}$ is 20000 $h^{-1}$, see fig. 4.

$t = 1/V_{sp} = 1/20000\ h^{-1} = 3600/20000\ sec^{-1}$, thus

$$K = -[20000 \ln(1 - X)]/3600. \tag{5}$$

Based on the conversion of COS ($X$), the reaction rate constant ($K$) was determined.

As shown in fig. 5, the relation between activity and the content of alkali metal oxides is slightly different from that of the alkali earth metal oxides. It was observed that there is a linear function between the activity and the content of alkali metal oxides when the content is relatively low. On the other hand, most

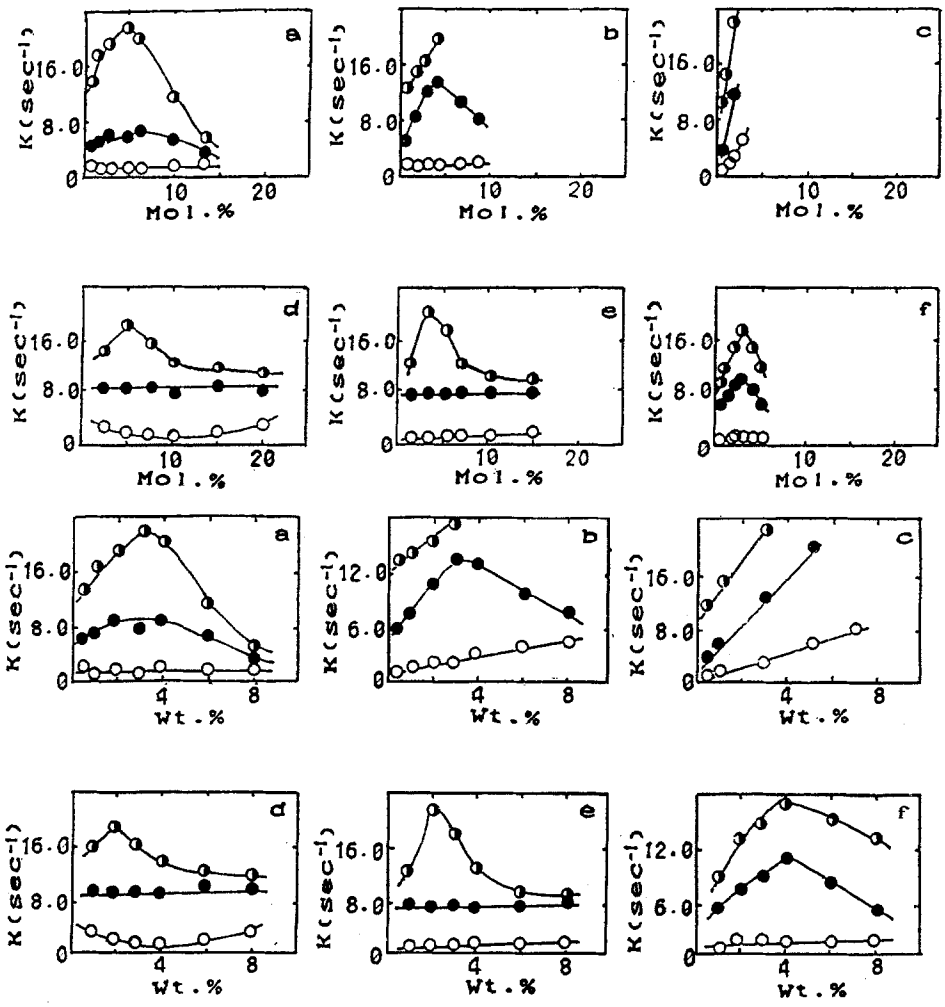


Fig. 5. Activity plot for COS hydrolysis over catalysts. a. $Na_2O/\gamma\text{-}Al_2O_3$; b. $K_2O/\gamma\text{-}Al_2O_3$; c. $Cs_2O/\gamma\text{-}Al_2O_3$; d. $MgO/\gamma\text{-}Al_2O_3$; e. $CaO/\gamma\text{-}Al_2O_3$; f. $BaO/\gamma\text{-}Al_2O_3$; ○ 55 °C, ● 70 °C, ◑ 80 °C.

catalyst series present a peak activity at various oxide contents. However, no peak activity was observed over $Cs_2O/\gamma\text{-}Al_2O_3$ at all operation temperatures. It is likely that a peak activity exists at $Cs_2O$ content of more than 8% (wt.%), due to the relatively large atomic number of Cs.

## SURFACE OXIDE COVERAGE

The surface oxide coverage was shown in table 1. Assuming that at relatively low coverages oxides cover the surface of alumina in a monolayer, each ion covering independently of others. The surface oxide coverage ($Y$) for $M_2O$ can be

Table 1
Surface oxide coverage ($Y$)

| Temp. (°C) | Oxide content at peak activity (wt.%(Mol.%)) | | | | | |
|---|---|---|---|---|---|---|
| | $Na_2O$ | $K_2O$ | $Cs_2O$ | MgO | CaO | BaO |
| 55 | / | / | > 8.0 (3.0) | * | / | / |
| 70 | 3.0 (5.0) | > 1.0 (1.1) | > 3.0 (1.1) | / | / | 4.0 (2.7) |
| 80 | 3.0 (5.0) | > 2.0 (2.2) | > 3.0 (1.1) | 2.0 (5.1) | 2.0 (3.7) | 4.0 (2.7) |
| $Y$ | 17.0–22.7 | 21.2 | 19.7 | 10.5 | 9.5–14.25 | 6.25 |
| Average (%) | | 20.1 | | | 10.3 | |

* Minimum activity was observed, explained later.

calculated as follows,

$$Y = \left\{(L/M) * Af * \left[2\pi(d_{m^+})^2 + \pi(d_{O^{2-}})^2\right]\right\}/(S_0 * 10^{20})\%$$

$$= 93.211L\left[2(d_{m^+})^2 + (d_{O^{2-}})^2\right]/M\% \text{ (for } M_2O/\gamma\text{-}Al_2O_3). \quad (6)$$

Similarly we have the surface oxide coverage ($Y$) for MO,

$$Y = 93.211L\left[(d_{m^{2+}})^2 + (d_{O^{2-}})^2\right]/M\% \text{ (for } MO/\gamma\text{-}Al_2O_3) \quad (7)$$

where $Y$: Surface oxide coverage %

93.211: $Af * \pi/S_0 * 10^{20}$

$Af$: Avogadro's constant $6.023 * 10^{23}$

$S_0$: $\gamma$-$Al_2O_3$ surface area, 203 $m^2/g$

$L$: Oxide content at peak activity (wt.%)

$d_{m^+}$, $d_{m^{2+}}$, $d_{O^{2-}}$: $M^+$, $M^{2+}$, $O^{2-}$ ionic radius ($10^{-1}$ nm) [8]

$M$: Molecular weight of oxide.

As seen in table 1, metal oxide contents at peak activity with smaller ionic radii (Na, Mg) are about 5% (Mol.%). However, they decrease when the ionic radius increases, whereas the surface oxide coverages remain more or less the same. Peak activities are about 20.1% for alkali metal oxides and 10.3% for alkali earth metal oxides.

## COMPENSATION EFFECT

The occurrence of compensation effect has been widely reported in many and diverse surface reactions [9]. According to the Arrhenius equation

$$K = A \exp(-E/RT), \quad (8)$$

where $A$: Reaction frequency factor or pre-exponential factor

$E$: Activation energy.

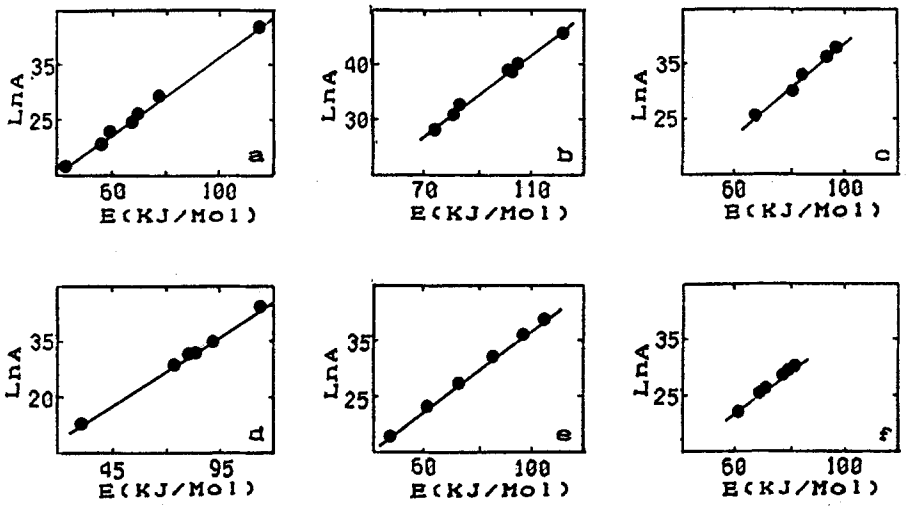


Fig. 6. Compensation effect for COS hydrolysis. a. $Na_2O/\gamma\text{-}Al_2O_3$; b. $K_2O/\gamma\text{-}Al_2O_3$; c. $Cs_2O/\gamma\text{-}Al_2O_3$; d. $MgO/\gamma\text{-}Al_2O_3$; e. $CaO/\gamma\text{-}Al_2O_3$; f. $BaO/\gamma\text{-}Al_2O_3$.

The compensation effect is usually expressed by

$$\ln A = bE + C, \tag{9}$$

where $b$ and $C$ are constants.

The Arrhenius equation can also be expressed as

$$\ln K = \ln A - (E/RT). \tag{10}$$

From (5) and (10), we have

$$\ln - \{[20000 \ln(1 - X)]/3600\} = \ln A - (E/RT), \tag{11}$$

the values of $X$, $T$ are observable. Two parameters $E$ and $A$ ($\ln A$) for every catalyst can be estimated from a set of eq. (11) by means of the regression method.

By studying the reaction rate constants ($k$) at various temperatures, it was found that the compensation effect exists in all six catalyst series. That is, the activation energy ($E$) increases along with the increase of pre-exponential factor ($A$), see fig. 6.

In recent years there have been many attempts to explain this compensation effect. Some of the theories have dealt with the number and nature of the active sites [10–12]. A possible general explanation was presented by Conner [13,14] by relating the entropy of transition to a change in the energy levels of the transition state. Considering that the compensation effect is found for both homogeneous and heterogeneous reactions and explanations of the compensation effect due to specific surface properties might not interpret the phenomena fully, Conner's theory would be an approach to give insight into the fundamental explanations.

In this study we assume an energetically heterogeneous catalyst surface, which was first put forth by Constable [15]. Also we may assume that the reaction mechanism remains unchanged for all catalysts studied.

We have eq. (8), thus the overall rate constant is given by

$$K = \sum_j A * N_i * \exp(-E_i/RT) \tag{12}$$

where $N_i$: Number of the $i$th type active sites upon which the activation energy for

COS hydrolysis is $E_i$.

$E_i$: Activation energy of the reaction on sites of the $i$th kind.

The distribution function may be expressed by

$$\mathrm{d}[N(E)]/\mathrm{d}E = a * \exp(E/b), \tag{13}$$

where $a$ is constant for a one catalyst system. Thus eq. (12) is replaced by integration between the lower limit $E_1$ and the upper limit $E_2$.

$$K = \int_{E_1}^{E_2} A * [\mathrm{d}N(E)]/\mathrm{d}E * \exp(-E/RT)\,\mathrm{d}E$$

$$= \int_{E_1}^{E_2} a * A * \exp\{-E[(1/RT) - (1/b)]\}\,\mathrm{d}E. \tag{14}$$

If the distribution of the activation energy is broad, $\exp\{-E_2[(1/RT) - (1/b)]\}$ may be neglected in comparison with $\exp\{-E_1[(1/RT) - (1/b)]\}$, and we may write

$$K = a * A * \{1/[(1/RT) - (1/b)]\} * \exp\{-E_1[(1/RT) - (1/b)]\}. \tag{15}$$

Eq. (15) shows that the compensation effect is operating. That is, one of the terms increases and another of the terms decreases.

Experimental data are well on one line for every catalyst series. Fig. 6 gives very good linear relationship.

The explanation may be that there is an exponential energy distribution on the catalyst surface. Thus the higher activity is not related to the lower activation energy, see fig. 6.

When comparing the compensation effect equation ($\ln A = bE + C$) and the Arrhenius relation ($\ln A = E/RT + \ln K$), we define an isokinetic temperature $T_s$ by equation, $b = 1/RT_s$, where the $K$'s are identical for all values of $E$, see fig. 7. At $T_s$ the relative rates of reactions within a group of catalysts undergo an inversion, and $T_s$ may or may not be experimentally accessible. Fig. 7 is a theoretical activity plot within a group of catalysts, if the compensation effect occurs.

From the Arrhenius equation [$K = A * \exp(-E/RT)$], we can see that increases in both $E$ and $A$ at the same time have the effect of minimizing changes

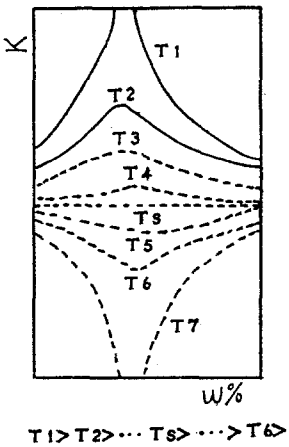


Fig. 7. Theoretical activity plot within a group of catalysts. Reaction rate constant ($K$) vs. $M_2O$, $MO/Al_2O_3$ (wt%).

in the rate constant $K$. Thus, for two catalysts we have

$$K_1/K_2 = A_1/A_2 * \exp[(E_2 - E_1)/RT]. \tag{16}$$

Considering the two terms of eq. (16), that is, $A_1/A_2$ and $\exp[(E_2 - E_1)/RT]$ obviously the importance of $\exp[(E_2 - E_1)/RT]$ will be decreased along with the increase of temperature, while the term of $A_1/A_2$ is essentially the same at various temperatures. Thus at higher temperatures term $A_1/A_2$ contributes much more to $K_1/K_2$. On the other hand, term $\exp[(E_2 - E_1)/RT]$ becomes more important at lower temperatures. A certain temperature $T_s$ exists where the two terms act as a counterbalance to each other, namely, $K_1/K_2 = 1$. At the isokinetic temperature $T_s$ the rate constants are equal for one group of catalysts in spite of the changes of the metal oxide loading. At $T > T_s$ there are maxima in activity, while at $T < T_s$ minimum values of reaction constant appear, see fig. 7.

We have

$$\ln A = (E/RT_s) + \ln K_0 \tag{17}$$

where $K_0$ is constant for all $A$ and $E$ at $T_s$.

When $E = 0$, we have

$$\ln A = \ln K_0 = C. \tag{18}$$

Thus we may write for all values of $E$,

$$\ln A = bE + C = (E/RT_s) + \ln K_0. \tag{19}$$

Equation (19) was used as objective function. To regress the experimental data, we have $T_s$, $K_0$ and $b$ for every catalyst series, see table 2.

Table 2
Parameters of compensation effect for COS hydrolysis

| Catalysts | $T_s$ (°C) | $K_0$ ($sec^{-1}$) | $b$ (kJ/mol) | $r$ | $1/b$ (mol/kJ) | $d_m$ ($10^{-1}$ nm) | $\phi$ |
|---|---|---|---|---|---|---|---|
| $Na_2O/\gamma\text{-}Al_2O_3$ | 64.1 | 4.50 | 0.357 | 0.999 | 2.80 | 0.95 | 10.6 |
| $K_2O/\gamma\text{-}Al_2O_3$ | 57.3 | 3.32 | 0.364 | 0.998 | 2.75 | 1.33 | 7.56 |
| $Cs_2O/\gamma\text{-}Al_2O_3$ | 28.8 | 0.28 | 0.398 | 0.997 | 2.51 | 1.69 | 5.95 |
| $MgO/\gamma\text{-}Al_2O_3$ | 70.4 | 7.63 | 0.350 | 0.999 | 2.86 | 0.65 | 30.6 |
| $CaO/\gamma\text{-}Al_2O_3$ | 65.8 | 4.81 | 0.355 | 0.999 | 2.82 | 0.99 | 19.9 |
| $BaO/\gamma\text{-}Al_2O_3$ | 57.2 | 2.71 | 0.364 | 0.996 | 2.75 | 1.35 | 14.9 |

It was shown that $T_s$ and $K_0$ decrease along with the increase of atomic number. The catalytic activity changes as follows,

$Cs_2O/\gamma\text{-}Al_2O_3 > K_2O/\gamma\text{-}Al_2O_3$, $BaO/\gamma\text{-}Al_2O_3 > Na_2O/\gamma\text{-}Al_2O_3$,

$CaO/\gamma\text{-}Al_2O_3 > MgO/\gamma - Al_2O_3$.

It explains why the activities of all prepared catalysts at 55°C almost did not change along with the oxide contents. In the case of $MgO/\gamma\text{-}Al_2O_3$ even the poisoning phenomenon was observed, see fig. 5d, and a minimum activity existed. This phenomenon may be the result of the highest isokinetic temperature $T_s$ (70.4°C) for $MgO/\gamma\text{-}Al_2O_3$.

Compensation effect is an interesting, yet still unresolved phenomenon. The relationships described above are useful in estimating rate parameters if data is lacking. Fig. 5 may be looked upon as part of fig. 7. Unfortunately the lack of adequate theories behind the correlations makes the acquisition of experimental results a necessity in order to substantiate the estimates.

## CORRELATION BETWEEN ($K_0$, $1/b$) AND METAL IONIC RADIUS ($d_m$) SEE TABLE 2 AND FIG. 8

There is a good linear relation between $K_0$ and $d_m$, regress it, we have

$$K_0 = 11.439 - 6.5189\, d_m \quad (r = 0.981). \tag{20}$$

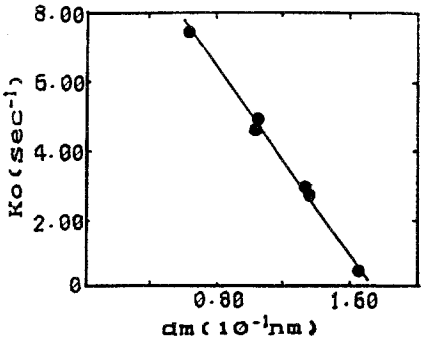


Fig. 8. Correlation between $K_0$ and $d_m$.

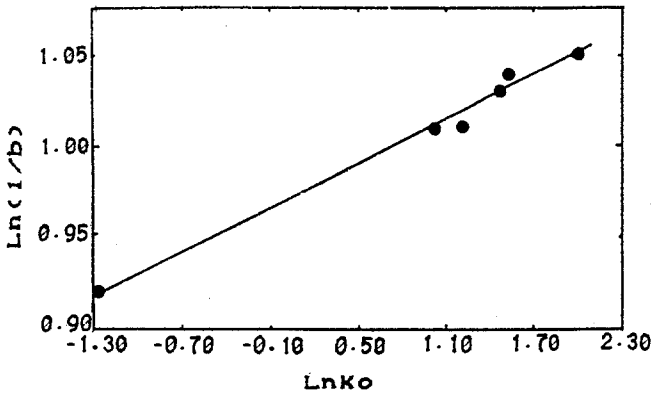


Fig. 9. Correlation between $K_0$ and $1/b$.

Similarly, see fig. 9, we have

$$\ln(1/b) = \ln 2.6382 + 0.039577 \ln K_0 \quad (r = 0.997). \tag{21}$$

$K_0$ is a compensation effect parameter. Its value equals reaction frequency factor or pre-exponential factor ($A$) when $E = 0$, see eq. (17). $1/b$ is the energy distribution exponential factor. Both factors are related to the number of active sites on the catalyst surface. If we assume that the active sites are mainly related to the metal ions, and that the number of active sites to the ionic radius ($d_m$), then $K_0$ and $1/b$ will be related to $d_m$. The experimental results support this assumption.

Fig. 10 shows the relation between ionic potential $\phi$ and $K_0$. There are two parallel lines for alkali metal series and alkali earth metal series. The ionic electric charge and the ionic radius may be the main elements to have an effect on the parameters ($K_0$, $T_s$, $b$) of the compensation effect for COS hydrolysis.

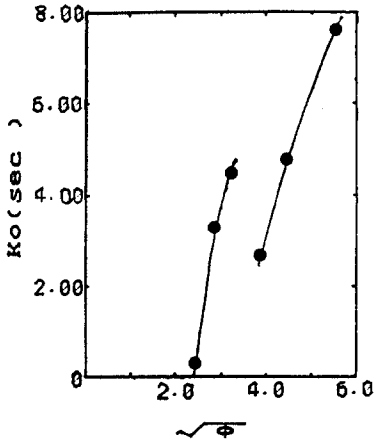


Fig. 10. Correlation between $K_0$ and $\phi$.

**Acknowledgment**

Many helpful suggestions by Zhang Qinling are greatly appreciated. Excellent technical assistance was provided by Shi Xinhua.

## References

[1] A.Y. Vincont Chen and I.G. Dalla Lana, Can. J. Chem. Eng. 56 (1978) 751.
[2] Z.M. Geoge, J. Catal. 32 (1974) 261.
[3] S. Namba and T. Shiba, Kogyo Kagaku Zasshi 71 (1968) 93.
[4] R. Fiedorow, R. Leaute and I.G. Dalla Lana, J. Catal. 85 (1984) 339.
[5] Zhang Qinling and Guo Hanxien, Cuihuaxuebao 9 (1988) 14.
[6] Zhang Qinling and Guo Hanxien, ibid. 9 (1988) 131.
[7] L.A. Pursglove and H.W. Wainwright, Anal. Chem. 26 (1954) 11.
[8] J.A. Dean, *Lange's Handbook of Chemistry*, 12th Edition, (1979) 3.
[9] A.K. Galwey, Advances in Catalysis 26 (1977) 247.
[10] G.M. Schwab, J. Catal. 84 (1983) 1.
[11] G.C. Bond, Catalysis 6 (1983) 234.
[12] A.K. Galwey, J. Catal. 84 (1983) 270.
[13] W.C.J. Conner, J. Catal. 78 (1982) 238.
[14] W.C.J. Conner, J. Catal. 84 (1983) 273.
[15] F.H. Constable, Proc. Roy. Soc. (London) Ser. A108 (1925) 355.